Preparation and thermal characterization of oxalic acid dihydrate/bentonite composite as shape-stabilized phase change materials for thermal energy storage

Lipeng Han[1,2], Shaolei Xie[1], Jinhe Sun[1,3,*] and Yongzhong Jia[1,4,*]

[1] Key Laboratory of Comprehensive and Highly Efficient Utilization of Salt Lake Resources, Qinghai Institute of Salt Lakes, Chinese Academy of Sciences, Xining, 810008, China
[2] University of Chinese Academy of Sciences, Beijing, 100049, China

E-mail: [3,*]jinhesun@163.com, [4,*]jiayzh@hotmail.com

Abstract. Oxalic acid dihydrate (OAD) which has very high initial phase transition enthalpy is a promising phase change material (PCM). In this paper, shape-stabilized composite PCMs composed of OAD and bentonite were prepared by a facile blending method to overcome the problem of leakage. FT-IR results indicated the interactions between OAD and bentonite, such as the capillary force and the hydrogen bonding, resulting in the confined crystallization process. As a result, the OAD was confined to be amorphous. The thermogravimetric analysis and scanning electron microscope results showed that sample had the best coating effect when the amount of bentonite was 17.7%. The differential scanning calorimetry analyses demonstrated that a decrease in the OAD content was accompanied by a continuous decrease in the melting point and phase change enthalpy of the composites.

Keywords: phase change materials, thermal properties, oxalic acid dehydrate, bentonite

1. Introduction

Heat storage is used to close the temporal gap between thermal energy production and energy demand. In many cases, it is the prerequisite for the utilization of waste heat in periodic industrial processes and the connection of renewable energy sources (especially solar energy) to continuous thermal loads. The application of phase change materials (PCMs) is one possible heat storage technology. PCMs are functional materials for thermal energy storage by storing and releasing amount of latent heats during their phase change processes [1]. In recent years, due to high energy storage density and latent heat property, small temperature variation from storage to retrieval, and repeatable utilization property, PCMs have become a hotspot in the fields of electronics cooling [2,3], solar power generation [4,5], waste heat utilization [6,7] and aerospace applications [8], etc.

PCMs can be divided into inorganic or organic compounds. The latent heat value of inorganic PCMs is approximately twice as high as the latent heat value of organic PCMs; in addition, inorganic PCMs are commercially available and fairly inexpensive [9-11]. Oxalic acid dihydrate (OAD) is low manufacturing cost and wide usage. In OAD, alternating acid and water molecules that act both as hydrogen-bond donors and acceptors [12]. OAD needs a lot of energy to break the hydrogen-bond in the melting process. Therefore, OAD has a very high heat of fusion of 370 $J \cdot g^{-1}$ [13], which is a very

promising PCM in TES for applications such as industrial waste heat recovery or solar energy storage systems [14-17]. This is why authors of this paper have considered the use of OAD as a PCM. However, OAD has large degradations of thermophysical properties over time. The melting point of OAD is 101°C (onset value) higher than the boiling point of water. When OAD is heated to melt, it is easy to produce high pressure caused by the water steam. High pressure not only results in severe leakage but also puts forward advanced requirements of the equipment. Meanwhile, actual applications of OAD inevitably face the enduring problems: relatively strong corrosivity. Some researchers have demonstrated that PCMs can be encapsulated by using porous materials to overcome these problems [18].

Bentonite has strong hygroscopicity and swelling properties, can be dispersed in an aqueous medium into gel shape and slurry. Bentonite is an absorbent aluminum phyllosilicate, and its main uses are for drilling mud, binder, absorbent and as a groundwater barrier. Due to its nano-layer structures, high thermal conductivity and low cost, bentonite also can be used as the supporting material of shape-stabilized PCMs (ss-PCMs) [19,20].

In this paper, we aim to maximize impregnation of OAD between interlayer of bentonite, to reduce leakage problem. Therefore, we prepared OAD and bentonite composites with varying concentration of bentonite and subsequently investigated the effects of a variety of concentration of bentonite on the OAD composites as PCMs.

2. Experiments

2.1. Materials

In this investigation, oxalic acid dihydrate (purity 99.5%) and bentonite were purchased from Aladdin Chemistry Co. Ltd (China). Deionized water was prepared in the laboratory.

2.2. Preparation of OAD composites containing bentonite

The OAD composites containing bentonite were prepared using a simple blending method. 10 g OAD was mixed with different mass bentonite (0.5 g, 1 g, 1.5 g, 2 g or 2.5 g) in a round bottom flask. The components of the OAD/bentonite composites are listed in table 1. The resulting mixture was then heated at 105 °C and stirred for 30 min. 1 mL deionized water was added to make up the water that adhered to the vessel wall in the melting process. Finally, the OAD composites containing bentonite were obtained after cooling at room temperature. It was worth noting that bentonite was too many to form a homogeneous mixture when the addition amount was 2.5 g. Some bentonite particles agglomerated, resulting in non-uniform dispersion. Therefore, the maximum addition amount of bentonite was 2 g.

Table 1. Components of the prepared OAD/bentonite ss-PCMs.

Samples	Components	OAD mass fraction
ss-sample I	10.0 g OAD + 0.5 g bentonite	95.2%
ss-sample II	10.0 g OAD + 1.0 g bentonite	90.9%
ss-sample III	10.0 g OAD + 1.5 g bentonite	87.0%
ss-sample IV	10.0 g OAD + 2.0 g bentonite	83.3%

2.3. Characterization

The morphologies and microstructure of the obtained composite PCMs were investigated using a scanning electron microscope (SEM) instrument (JSM-5610LV). Fourier transform infrared (FT-IR) spectra were recorded using a Thermo Nicolet NEXUS FT-IR spectrometer. A resolution of 4 cm^{-1} and the average of 32 automated scans from 400 to 4000 cm^{-1} were used to obtain the FT-IR spectra. Thermal properties of the composite PCMs, such as melting and latent heats, were measured using a Mettler Toledo differential scanning calorimetry (DSC). Measurements were performed at 10 $K \cdot min^{-1}$ or 2 $K \cdot min^{-1}$ in heating procedure and cooling procedure in nitrogen atmosphere. The temperature accuracy was ±0.01 °C, and the heat flow repeatability was 0.2 μW. The thermal stability of the

composite PCMs was determined using a Netzsch STA 449F3 at a scan rate of 5 $K \cdot min^{-1}$ under an atmosphere of nitrogen.

3. Results and discussion

3.1. Micro-morphology analysis of the ss-PCMs

Figure 1 shows the SEM images of pristine bentonite powders and the composites. From figure 1(a), bentonite is a crystal with layer structures. Moreover, one can observe the presence of a large space between discrete layers, which facilitates the intercalation of the solid-liquid PCMs. As illustrated from figure 1(b) to (c), grains are getting smaller. Meanwhile, it is easily to observe a homogeneous and rough morphology with increasing weight percentage of bentonite. OAD molecules can not only crystallize onto the bentonite surface but also in the inner pore of bentonite networks. According to the results of SEM, the ss-sample IV shows the best coating effect. This uniform encapsulation also indicates good cohesion between the inorganic matrix and OAD, which is due to the effect of capillary and surface tension force.

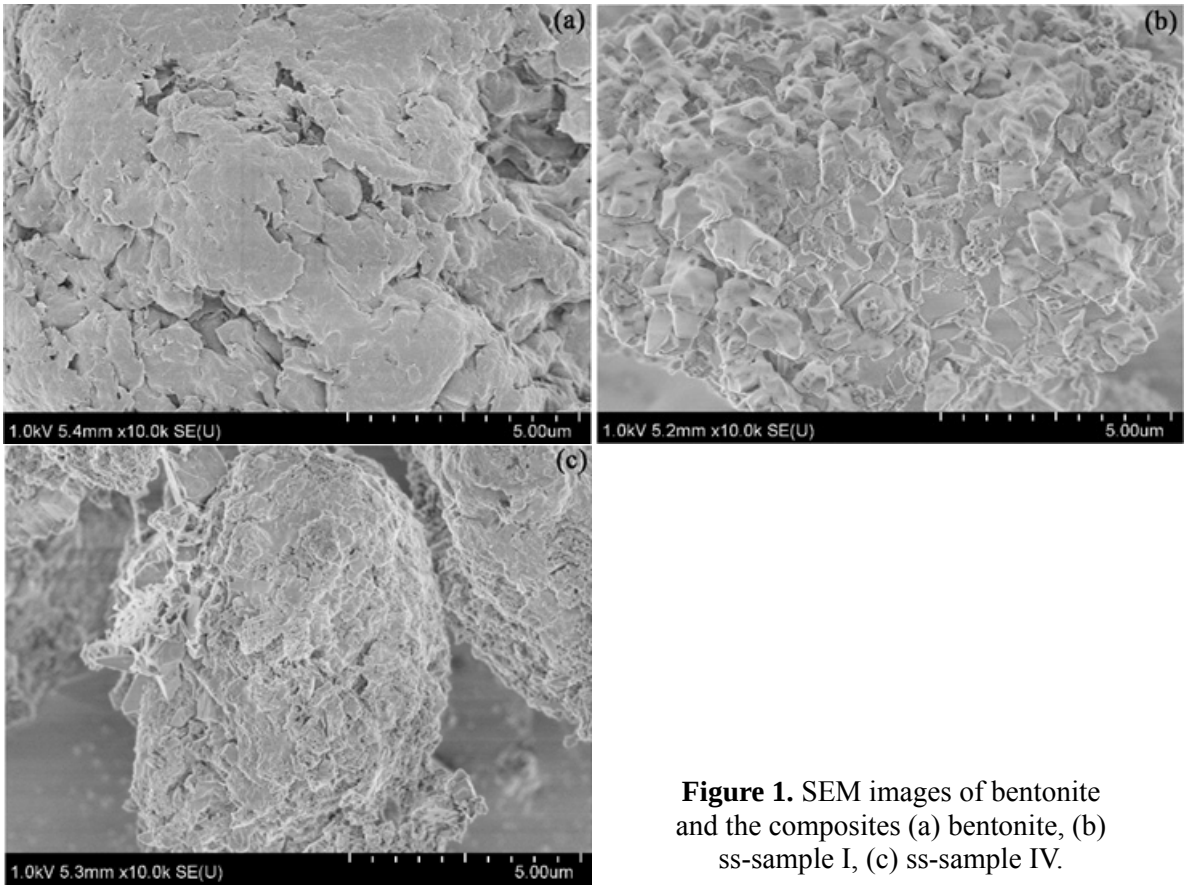

Figure 1. SEM images of bentonite and the composites (a) bentonite, (b) ss-sample I, (c) ss-sample IV.

3.2. FT-IR analysis of the ss-PCMs

FT-IR spectroscopy is usually used to investigate the specific interactions and material compositions in composites. Figure 2 displays the FT-IR spectra of pure OAD, bentonite and ss-PCMs. In the FT-IR spectrum of OAD, the peak at 1689 cm^{-1} represents the stretching vibration of the C=O group. The peaks at 3430 cm^{-1} signify O–H stretching vibration. The peak at 1254 cm^{-1} is assigned to the bending vibration of the −OH group. On the spectra of the bentonite, the peaks at 1043 cm^{-1} and 463 cm^{-1} represent O–H stretching vibration and Si–O–Si bending vibration, respectively.

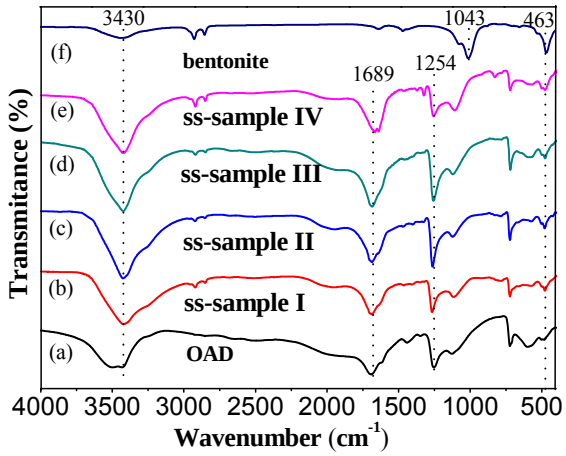

Figure 2. FT-IR spectrum of pure OAD, bentonite and the composite PCMs.

After comparing the spectra of the composite PCMs with those of bentonite and pure OAD, most absorption peaks of the main functional groups of OAD and the corresponding matrix also appear in the spectra of the ss-PCMs with only a slight shift. And no obvious new peaks are observed, which indicates that no new chemical bonds generate between OAD and the matrix. The frequency shift of the functional group indicates that there are some interactions between OAD and the supporting materials, which can prevent the leakage of the melted PCMs from the supporting materials. Due to the nano-layer structure of bentonite, there is a capillary force between melt OAD and bentonite in ss-PCMs [21,22]. Meanwhile, The FT-IR results suggest that there are C=O and O–H groups in both OAD and bentonite. Therefore, the hydrogen bonds infer from the frequency shifts of the functional group also exist between OAD and the porous materials.

3.3. Thermal behavior of OAD/bentonite ss-PCMs

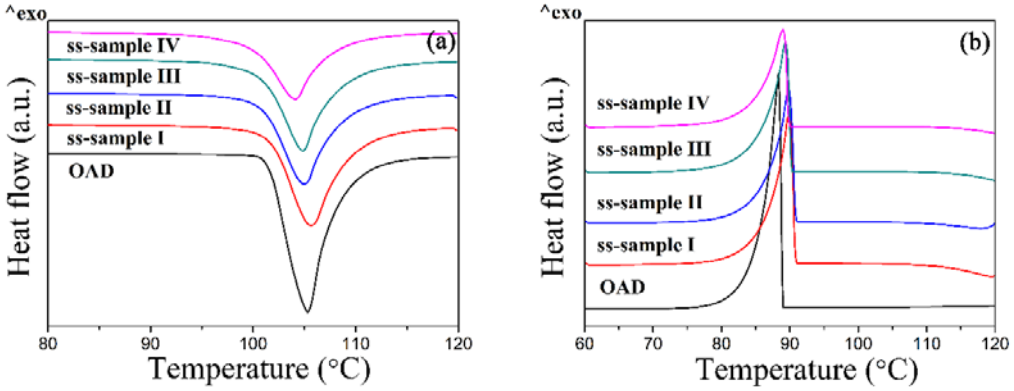

Figure 3. DSC thermograms of OAD and OAD/bentonite composited PCMs with the different amount of OAD components
(a) heating process at a rate of 10 k·min^{-1}, (b) cooling process at a rate of 10 k·min^{-1}.

The phase change temperature and latent heat of composites are measured with the DSC technique. Figure 3(a) and (b) demonstrate the heating and cooling DSC curves of pure OAD and composites with various OAD weight fractions at a heating and cooling rate of 10 K min^{-1}, and the corresponding data deduce from the DSC curves are listed in table 2. Clearly, all the composites exhibit similar curves as pure OAD, indicating that the OAD acts as the PCM during the melting process. However, the phase change characteristics of the OADs are affected by adding bentonite. As listed in table 2, the onset melting (T_{mo}) temperature shifts slightly from 101.2 °C for pure OAD to around 99.5 °C for the composites. This phenomenon can be ascribed to two reasons. On the one hand, the porous bentonite

network in the composites provides heat conduction path in the OAD, which improves the thermal conductivity of OAD and consequently accelerates the phase change speed of the composites [23, 24]. On the other hand, bentonite is the impurity for OAD and can destroy the perfect crystallization, so the defects of crystal lattices increase, which cause the crystals can be damaged at low temperature [25].

In addition, the areas of the endothermic and exothermic peaks decrease significantly when OAD is incorporated into bentonite. Compared with pure OAD, the latent heat of OAD/bentonite composites is in the range of 205.8–287.7 $J \cdot g^{-1}$, which is lower than ideal latent heat which is 372.7 $J \cdot g^{-1}$. The decrease of the latent heat of the composite PCMs cannot be attributed to the lower fraction of OAD alone. Another factor is the blending of mesoporous matrices interferes with the crystallization of OAD. The interaction between OAD and its supports may keep OAD from crystallizing and influence the thermal properties of the composites and result in the smaller enthalpy. Perhaps fast heating and cooling rates of 10 $k \cdot min^{-1}$ make the OAD of the composites in the inner pore of bentonite networks fail to fully melt and crystallize. Extra measurements are then completed at a lower heating and cooling rate of 2 $k \cdot min^{-1}$. Figure 4(a) and (b) show that the thermal behaviour of composited PCMs at the heating and cooling rates of 2 $k \cdot min^{-1}$ is close to the former measurements. Onset melting (T_{mo}), degree of supercooling and phase change enthalpy only have a little change. Therefore, the speed of heating and cooling has moderate effect on the thermal behavior of the composites.

Table 2. Thermographic data of OAD and OAD/ bentonite composited PCMs.

samples	10 $k \cdot min^{-1}$				2 $k \cdot min^{-1}$			
	T_{mo} (°C)	ΔH_m (J g^{-1})	T_{co} (°C)	ΔH_c (J g^{-1})	T_{mo} (°C)	ΔH_m (J g^{-1})	T_{co} (°C)	ΔH_c (J g^{-1})
pure OAD	101.2	372.7	89.1	362.0	100.2	371.9	90.4	363.2
ss-sample I	101.2	287.7	91.0	286.7	99.6	291.0	93.4	290.8
ss-sample II	100.6	267.9	91.0	261.3	99.1	266.1	92.8	263.1
ss-sample III	100.4	255.4	90.4	251.0	98.8	250.9	92.6	249.7
ss-sample IV	99.5	205.8	90.0	202.5	98.2	201.0	91.5	195.8

We compare the thermal properties of the prepared composite PCM in this study with other composite PCMs in the literatures in table 3. It can be remarkably noted that the prepared OAD/bentonite composite PCM has high latent heat and appropriate phase change temperature. It indicates that the prepared composite PCM has good thermal energy storage potential.

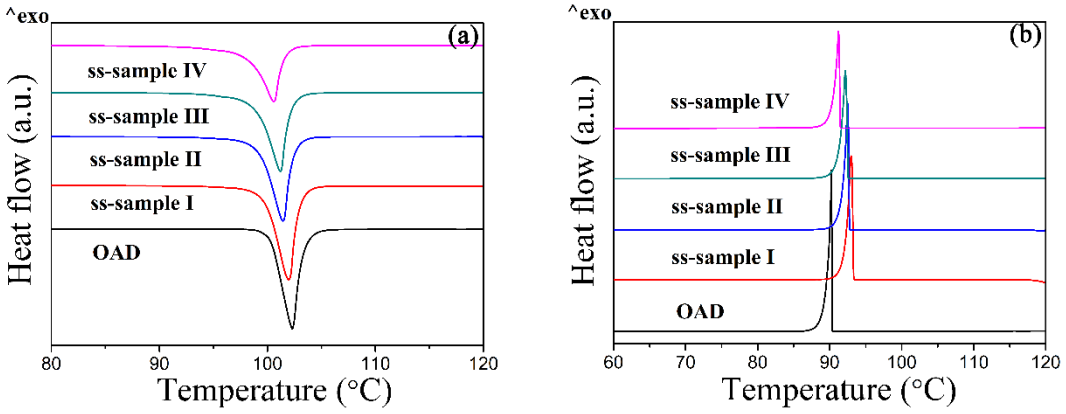

Figure 4. DSC thermograms of OAD and OAD/bentonite composited PCMs with the different amount of OAD components
(a) heating process at a rate of 2 $k \cdot min^{-1}$, (b) cooling process at a rate of 2 $k \cdot min^{-1}$.

Table 3. Thermal characteristics of some composite PCMs in literature.

Material/mass/%	Melting point (°C)	Latent heat ($J \cdot g^{-1}$)	Reference
Myristic acid (50%)/bentonite (50%)	53.2	54.5	[20]
Capric-myristic acid (20 %)/vermiculite (80%)	19.7	27.0	[26]
PEG (45 %)/diatomite (45 %)/EG (10 %)	27.7	88.2	[27]
$CaCl_2 \cdot 6H_2O$ (50%)/EG (50%)	29.9	88.5	[28]
Paraffin (72 %)/SiO_2 (20.8 %)/EG (7.2 %)	27.7	104.4	[29]
Paraffin(60 %)/HDPE(15 %)/(APP/PER/MA)25 %	51.7	81.5	[30]

3.4. Thermal stability of the OAD/bentonite composite PCMs

The OAD and the various OAD/bentonite composites are verified using thermogravimetric (TG) analyses in order to understand the thermal stability of them. Figure 5 shows TG curves of pure OAD and the composite PCMs. As can be seen from the curves, the mass loss of OAD and the composites starts at 70 °C and ends at 92.6–100.0 °C due to the degradation of crystal water in OAD. With the increase of the bentonite content, the mass loss becomes smaller and mass loss rate of composites also becomes lower when temperature is under 80 °C. It implies that the interactions between OAD and porous materials can provide composited PCMs with the good structure stable properties.

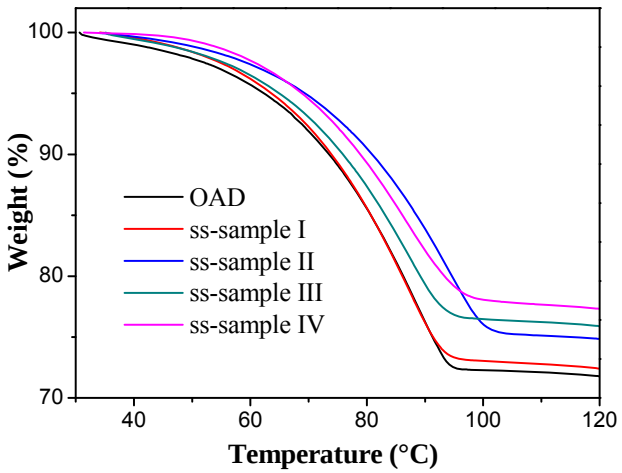

Figure 5. TG curves of OAD and the composites.

4. Conclusions

In this paper, the ss-PCMs composed of bentonite and OAD are prepared by a direct blending method. According to the results of SEM and TG, when the weight percentage of OAD in the composites is 83.3 wt.%, it can be found that OAD is preferably coated with bentonite. DSC data show a continuous lowering of the OAD melting point and phase change enthalpy with increasing bentonite content. According to the FT-IR results, interactions between OAD and bentonite, such as the capillary force and the hydrogen bonding, result in the confine crystallization process. OAD/bentonite composite with mass fraction of 83.3 wt.% OAD is promising candidates for heat storage application due to its moderate melting temperature, significant latent heat storage capacity and form-stable property.

Acknowledgement

Financial support from the National Natural Science Foundation of China (No. U1407205) and Youth Innovation Promotion Association of Chinese Academy of Sciences (No. 2015351) is gratefully acknowledged.

References

[1] Dutil Y, Rousse D, Salah N, Lassue S and Zalewski L 2011 *Renew. Sust. Energ. Rev.* **15** 112–130
[2] Khateeb S, Amiruddin S, Farid M, Selman J and Al-Hallaj S 2005 *J. Power Sources* **142** 345–353
[3] Sabbah R, Kizilel R, Selman J and Al-Hallaj S 2008 *J. Power Sources* **182** 630–638
[4] Steinmann W and Tamme R 2008 *J. Sol. Energy Eng.* **130** 1–5
[5] Pincemin S, Olives R, Py X and Christ M 2008 *Sol. Energy Mater. Sol. Cells* **92** 603–613
[6] Maruoka N and Akiyama T 2006 *Energy* **31** 1632–1642
[7] Kaizawa A, Kamano H, Kawai A, Jozuka T, Senda T, Maruoka, N and Akiyama T 2008 *ISIJ Int.* **48** 540–548
[8] Lafdi K, Mesalhy O and Elgafy A 2008 *Carbon* **46** 159–168
[9] Kenisarin M and Mahkamov K 2007 *Renew. Sust. Energ. Rev.* **11** 1913–1965
[10] Farid M, Khudhair A, Razack S and Al-Hallaj S 2004 *Energy Conv. Manag.* **45** 1597–1615
[11] Shin H, Park M, Kim H and Park S 2015 *Appl. Therm. Eng.* **75** 978–983
[12] Stare J and Hadži D 2014 *J. Chem. Theory Comput.* **10** 1817–1823
[13] Haillot D, Bauer T, Kröner U and Tamme R 2011 *Thermochim. Acta* **513** 49–59
[14] Naumann R and Emons H 1989 *J. Therm. Anal. Calorim.* **35** 1009–1031
[15] Gil A, Medrano M, Martorell I, Lázaro A, Dolado P, Zalba B and Cabeza L 2010 *Renew. Sust. Energ. Rev.* **14** 31–55
[16] Gutierrez A, Ushak S, Galleguillos H, Fernandez A, Cabeza L and Grágeda M 2015 *Appl. Energy* **154** 616–621
[17] El-Sebaii A, Al-Heniti S, Al-Agel F, Al-Ghamdi A and Al-Marzouki F 2011 Energy Conv. Manag. **52** 1771–1777
[18] Kadoono T and Ogura M 2014 *Phys. Chem. Chem. Phys.* **16** 5495–5498
[19] Li M, Wu Z, Kao H and Tan J 2011 *Energy Conv. Manag.* **52** 3275–3281
[20] Chen C, Liu X, Liu W and Ma M 2014 *Sol. Energy Mater. Sol. Cells* **127** 14–20
[21] Wang C, Feng L, Li W, Zheng J, Tian W and Li X 2012 *Sol. Energy Mater. Sol. Cells* **105** 21–26
[22] Sari A and Biçer A 2012 *Sol. Energy Mater. Sol. Cells* **101** 114–122
[23] Xia L and Zhang P 2011 *Sol. Energy Mater. Sol. Cells* **95** 2246–2254
[24] Wang X, Guo Q, Zhong Y, Wei X and Liu L 2013 *Renew. Energy* **51** 241–246
[25] Yuan Y, Li T, Zhang N, Cao X and Yang X 2016 *J. Therm. Anal. Calorim.* **124** 881–888
[26] Karaipekli A and Sari A 2009 *Sol. Energy* **83** 323–332
[27] Karaman S, Karaipekli A, Sarı A and Bicer A 2011 *Sol. Energy Mater. Sol. Cells* **95** 1647–1653
[28] Duan Z, Zhang H, Sun L, Cao Z, Xu F, Zou Y and Zhou H 2014 *J. Therm. Anal. Calorim.* **115** 111–117
[29] Li M, Wu Z and Tan J 2012 *Appl. Energy* **92** 456–461
[30] Zhang P, Hu Y, Song L, Ni J, Xing W and Wang J 2010 *Sol. Energy Mater. Sol. Cells* **94** 360–365